ACS OMEGA

Open Access

http://pubs.acs.org/journal/acsodf

Article

Enhanced Glycerolysis of Fatty Acid Methyl Ester by Static Mixer Reactor

Pakamas Chetpattananondh, Athcharaporn Tabtimmuang, and Kulchanat Prasertsit*

Cite This: *ACS Omega* 2024, 9, 39703−39714

Read Online

ACCESS | Metrics & More | Article Recommendations

ABSTRACT: This study investigates the synthesis of monoglycerides (MGs) and diglycerides (DGs) from glycerol (G) and fatty acid methyl ester (FAME) using a static mixer reactor (SMR), which combines a static mixer (SM) with a reactor tank. The SMR integrates Kenics static mixers (KSM) and low-pressure drop static mixers (LPDSM) with varying length-to-diameter ratios (L/D = 1.0 and 1.5). Keys glycerolysis parameters, including the G:FAME molar ratio of 2:1−3:1, 2−3 wt % potassium hydroxide (KOH), and reaction time of 30−90 min at 150 °C were systematically explored. The SMR design allows precise control over the reaction time without altering the feed flow rate or tube length and avoiding agitator leakage. The optimal operating conditions, determined through a face-centered central composite design, resulted in 71.35% MGs and 14.20% DGs at a 3:1 molar ratio of G to FAME, 3 wt % KOH, 60 min, and 150 °C using an LPDSM with an L/D of 1.5. In comparison, an LPDSM with an L/D of 1 achieved 79.28% MGs and 10.17% DGs under the same conditions. When applied to purified crude glycerol, these conditions yielded 61.09% MGs and 23.44% DGs. The study found that a lower L/D ratio improved the mixing efficiency but increased the pressure drop. The SMR demonstrated superior performance in glycerolysis compared with conventional stirred tank reactors and ultrasonic probe reactors, indicating its potential for enhanced industrial application.

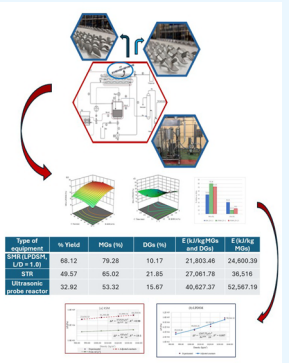

1. INTRODUCTION

Biodiesel is widely consumed because of several nations' clean energy regulations. Particularly, the amount of crude glycerol, a byproduct of biodiesel production, is around 10−20% of biodiesel.[1] As biodiesel production increases, a large accumulation of crude glycerol also increases.[2] Since crude glycerol contains impurities such as methanol, water, and fatty acids, it needs to be distilled before being used in various industries.[3] Glycerol is an oleochemical byproduct and one of the top 12 building blocks of biomass, according to the US Department of Energy.[4] However, due to the oversupply of crude glycerol and its high purification cost, the demand and price of crude glycerol tend to decrease.[3] Using crude glycerol as the reactant to produce monoglycerides (MGs) or monoacylglycerol and diglycerides (DGs) or diacylglycerol is the alternative process to increasing the value of crude glycerol. MGs and DGs can be used in combination or separately as emulsifiers in many industries. MGs are applied in food, cosmetics, drugs, polymers, resins, rubber, textiles, and other related products.[5,6] The demand for MGs most likely will grow every year.[7] Data Bridge Market Research analyses that the mono- and diglycerides and derivatives market, valued at $8.92 billion in 2022, will reach $16.44 billion by 2030, growing at a compound annual growth rate of 7.95% during the forecast period of 2023 to 2030.[8] DGs are a fat replacement due to their capability to inhibit the accumulation of body fat.[9−11] MGs are commercially available in two forms: high-purity distilled monoglycerides (95% MGs, 3−4% DGs, 0.5−1% free glycerol) and a combination of monoglycerides and diglycerides (45−55% MGs, 38−45% DGs, 8−12% triglycerides, and 1−7% free glycerol).[12]

Normally, about 40% of MGs and 50% of DGs are produced via glycerolysis in a stirred tank reactor which requires energy for agitation.[13] At low temperatures, the typical reaction between glycerol (G) and triglycerides (TGs) has little miscibility; hence a high temperature of 200−260 °C is necessary.[14] One constraint of high temperature monoglyceride (MG) synthesis is that the TGs employed must be saturated fatty acids. This is because unsaturated fatty acids can produce oxidation and isomerization events that result in undesirable chemicals. Adding organic solvents such as phenol and pyridine increases the solubility between G-TGs and reduces the reaction temperature.[15] However, such organic solvents are toxic, difficult to remove, and have high costs. Free fatty acids (FFAs) or waste oils can be used to synthesize MGs and DGs. However, glycerolysis of FFAs and waste oils is a slower reaction that takes more time and higher temperature than transesterification of fatty acid methyl esters (FAMEs).[16]

Received: May 23, 2024
Revised: July 5, 2024
Accepted: September 2, 2024
Published: September 12, 2024

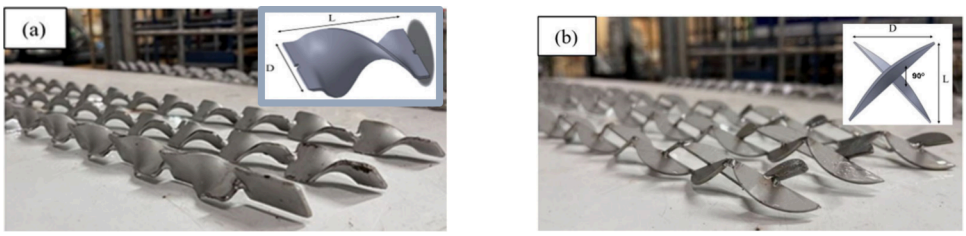

Figure 1. Studied static mixers: KSM (a) and LPDSM (b).

Furthermore, FAMEs are often more refined than FFAs and waste oils. The reaction between G and fatty acid methyl ester (FAME) has various benefits, including being less corrosive than fatty acid, having a lower hydrophobic character than triglyceride (TG), and being more miscible with glycerol. This allows for lower temperatures (120−230 °C) compared to TG transesterification (≈260 °C).[17]

Static mixers are now considered to be common equipment in the process sector. They are utilized in continuous processes as a cost-effective alternative to traditional agitation, since they provide equal or greater performance. Because there are no moving parts, motionless mixers often consume less energy and require less maintenance.[18] There are some reports on enhancing FAME production using static mixers,[19] but not for MG and diglyceride (DG) production. A static mixer (SM) is a mixing device that consists of a mixer element within a pipe to induce fluid mixing.[20] The mixer element forces the flow direction of each fluid along the circle of splitting and combining of fluid volume.[21] Because static mixers have no moving parts, they consume less energy and require less maintenance. SMs are used in various industries, including water treatment, biotechnology, and polymer production.[22] The fluid viscosity, density, and mixing intensity are factors for the mixer element selection. The Kenics static mixer (KSM) is a patented helical mixing device that guides material flows radially toward pipe sides and then back to the center. It is configured as a twisted-ribbon type (Figure 1a). Each part of the element was twisted and connected to another.[23] The low-pressure drop static mixer (LPDSM) is shown in Figure 1b. Each baffle of the LPDSM consists of two half-oval plates joined together with a perpendicular position to the next element.[24] Both Kenics and LPDSM give excellent mixing at low pressure and create a high flow rate even with low viscosity. KSM is one of the most widely used SM types[25] because it can induce radial and uniform mixing, even when operating within a laminar regime.[26] However, a static mixer is not ideal for lengthy reaction periods since it requires a very long pipe or a large volume of pipe.[27]

Mixing energy exists in the form of pressure in a static mixer. The pressure drop is the limiting element in selecting the mixer and a key consequence of static mixing, regardless of whether the material is delivered to the mixer via an external pump or gravity-fed.[28] There have been some studies on the static mixer pressure drop calculation for Newtonian and non-Newtonian fluids.[29,30] However, the influence of the mixer element area on the pressure drop has regrettably been disregarded in all of those works.

Response surface methodology (RSM) uses statistical tools to optimize processes based on several factors and understand their relationships. It reduces the quantity of data needed for evaluation, analysis, and optimization.[31] A full factorial experiment in which every possible value of each parameter is tested is not cost-effective. The fractional factorial approach, also known as face-centered central composite design (FCCD), was utilized, as it required fewer runs. The FCCD requires only three levels of each experiment variable, making it the simplest variety of central composite design (CCD) to carry out. FCCD is the least prone to corruption due to sources of experimental error associated with setup and operation.[32] There are a few works on optimizing the glycerolysis conditions for the production of MGs and DGs using RSM.[33,34] However, the feedstocks and process parameters are different from those in this study. According to the literature review, no studies on glycerolysis using a static mixer have been reported.

This study aimed to optimize the production of MGs and DGs via a static mixer coupled to a reactor tank (SMR). Glycerolysis conditions of FAME and pure glycerol were optimized using RSM and FCCD. The optimum conditions were also applied to purified glycerol. In addition, the numerical pressure drop correlation with respect to the effect of the mixer area of SM was proposed.

2. MATERIALS AND METHODS

2.1. Materials. FAME and crude glycerol were obtained from the Specialized R&D Center for Alternative Energy from Palm Oil and Oil Crops at the Faculty of Engineering, Prince of Songkla University. The gas chromatography (GC) examination of the FAME revealed a fatty acid composition ranging from C8:0−C24:1, with oleic acid (C18:1) and palmitic acid (C16:0) being the most abundant. The FAME has a similar fatty acid composition to most FAMEs derived from palm oil.[35] Commercial-grade pure glycerol (99% purity) was purchased from Thai Glycerine Co., Ltd. The chemical reactants used in the experiments were commercial-grade 95% potassium hydroxide (KOH) and 99.5% ethanol. KOH was selected as a catalyst, since it is a relatively inexpensive common industrial chemical utilized in the manufacturing of biodiesel, making it easily accessible and economical for large-scale production. Furthermore, the previous work found that KOH outperformed sodium hydroxide (NaOH) and magnesium oxide (MgO) in the synthesis of MGs.[35]

2.2. Equipment and Design Concept. Glycerolysis reaction is a slow process with a long interval (30−90 min). Normally, the retention time or resident time in SM can be adjusted by changing the flow rate or SM length, but both approaches have disadvantages. From fluid flow theory, changing the flow rate affects fluid flow patterns[22] while changing the length affects construction and layout. In addition, there is a lack of a degree of freedom to adjust both the flow rate and reaction time simultaneously. According to a rough estimate based on ideal plug flow behavior, retention time can be calculated by dividing the mixer volume by the flow rate.[27] A 90 min retention time requires 134 m of

https://doi.org/10.1021/acsomega.4c04858
ACS Omega 2024, 9, 39703−39714

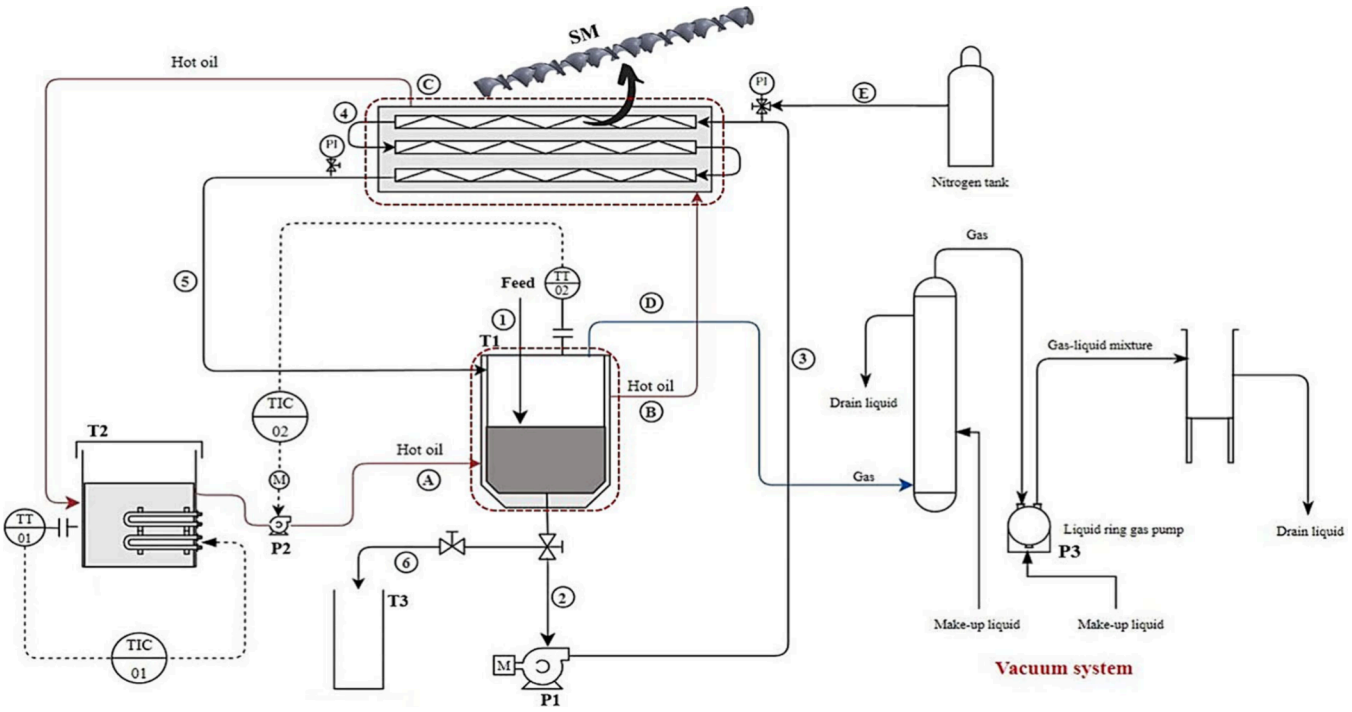

Figure 2. Schematic diagram of the experimental setup (T1: Reactor tank, T2: Hot oil tank, T3: Product tank, P1: Reactant circulating pump, P2: Hot oil-circulating pump, P3: Vacuum pump, SM: Static mixer).

Table 1. Experimental Variables and Response Variables for MGs and DGs Using KSM (L/D = 1.5) and LPDSM (L/D = 1.5)

	Experimental variables			Response variables[c]							
				KSM				LPDSM			
N[a]	Molar ratio (G:FAME)[b]	KOH (wt %)	Time (min)	Actual MGs (%)	Predicted MGs (%)	Actual DGs (%)	Predicted DGs (%)	Actual MGs (%)	Predicted MGs (%)	Actual DGs (%)	Predicted DGs (%)
1	3	2	90	42.01	41.88	16.12	16.32	54.61	55.00	19.98	19.88
2	2	2.5	60	30.68	30.60	18.73	18.39	55.97	56.02	19.10	18.49
3	2	3	30	22.89	23.10	12.74	12.55	51.18	50.61	13.85	13.96
4	3	3	30	42.84	42.78	25.85	26.51	68.13	68.46	16.16	15.75
5	2	2	90	36.78	36.92	20.30	19.65	48.91	48.62	25.59	26.03
6	2	3	90	21.44	21.15	11.09	11.79	52.82	53.16	25.49	25.53
7	3	2	30	8.87	9.24	2.72	2.03	51.95	51.43	20.05	20.02
8	2	2	30	16.63	16.65	12.91	13.39	41.97	42.45	16.36	16.38
9	3	3	90	53.14	53.20	34.27	33.80	68.87	68.42	17.53	17.54
10	2.5	2.5	60	43.46	43.44	24.30	23.32	65.64	65.33	18.59	18.12
11	2.5	2.5	60	42.92	43.44	22.30	23.32	66.32	65.33	17.90	18.12
12	2.5	3	60	45.09	45.17	21.82	21.12	65.85	66.64	18.14	18.43
13	2.5	2.5	60	43.16	43.44	23.30	23.32	64.3	65.33	17.85	18.12
14	2.5	2.5	60	43.46	43.44	24.30	23.32	65.31	65.33	18.59	18.12
15	2.5	2.5	60	43.56	43.44	22.30	23.32	66.12	65.33	17.51	18.12
16	2.5	2.5	90	47.45	47.68	28.79	29.01	63.64	63.65	21.85	21.46
17	2.5	2	60	36.69	36.29	12.15	12.81	55.9	55.85	21.15	20.81
18	3	2.5	60	43.16	42.92	23.41	23.71	67.45	68.14	15.75	16.31
19	2.5	2.5	30	32.89	32.34	22.51	22.24	60.29	60.58	15.44	15.74

[a]Run Number. [b]G:FAME, Molar ratio of G to FAME. [c]KSM, Kenics Static Mixer; LPDSM, Low-Pressure Drop Static Mixer; MGs, Monoglycerides; DGs, Diglycerides.

SM or a flow rate of 7.03 × 10−6 m^3/s. It is impractical to construct and operate this incredibly long SM and control this low flow rate. The SMR consisting of the SM and reactor tank offers the advantage of flexibility of operation. The retention time can be varied without the need to change the flow rate or SM length. The static mixer coupled with the reactor tank (SMR) shown in Figure 2 consists of a set of three 1 m-long SMs placed parallel in the 13 L tank containing hot oil to control the reaction temperature connected to a 13 L reactor tank to increase reaction time.

FAME, G, and KOH catalysts dissolved in ethanol (with a ratio of 1:5 w/w) were fed into the reactor tank (Point 1). Nitrogen gas was fed into the SMR (Point E) to prevent the oxidation process. A temperature controller coupled to a hot

https://doi.org/10.1021/acsomega.4c04858
ACS Omega 2024, 9, 39703−39714

oil tank T2 and a hot oil pump P2 kept the temperature within the reactor tank T1 constant at each examined setting (140−215 °C). The hot oil temperature in the hot oil Tank T2 was kept constant at 160 °C. Pump P2 circulated hot oil in the jacket (Points A−C). The vacuum system (Point D) was operated to control the vacuum condition inside reactor tank T1 at 0.3 bar. When the reaction temperature inside reactor tank T1 reached the set point, pump P1 was turned on. A mixture of fed raw materials was circulated throughout the SM (Points 2−5) and reactor tank until the reaction time was complete. During the reaction process, a pressure drop was measured with a pressure gauge PI installed between the inlet and outlet of the SM (on top view). After the end of the reaction, pumps P1, P2, and P3 were turned off, the hand valve (point 6) was opened, and the product was kept in the cooling tank T3 to cool to 60 °C within 10 min.

2.3. Glycerolysis Using SMR. Pure glycerol (G) and FAME were used as the reactants for glycerolysis. The effect of temperature was studied in the range of 140−215 °C keeping the molar ratio of G:FAME at 2.5:1, 3 wt % KOH of G, and reaction time 60 min. After the optimal temperature was selected, other parameters including G:FAME molar ratio (X_1) of 2:1−3:1, KOH concentration (X_2) of 2−3 wt % of G, and reaction time (X_3) of 30−90 min were studied using RSM and FCCD.

Nineteen experimental settings of each type of mixing element with L/D = 1.5 as shown in Table 1 were carried out with five replications at the center points. The quadratic polynomial regression model as shown in eq 1 was assumed to predict the responses.

$$Y = \beta_0 + \sum_{i=1}^{k} \beta_i X_i + \sum_{i=1}^{k} \beta_{ii} X_i^2 + \sum \sum_{i<j} \beta_{ij} X_i X_j + \varepsilon \quad (1)$$

where Y represents the response and β_0, β_i, β_{ii}, and β_{ij} are constant, linear, quadratic, and interaction coefficients, respectively. X_1, X_2, ..., X_k represent the coded values of the input, k represents the number of studied factors, and ε represents the experimental error ascribed to Y.

The analysis of variance (ANOVA) approach was used to assess the model's relevance and applicability by considering the regression parameters such as the coefficient of determination R^2, F-value, p-value, and lack-of-fit. The confidence level was set at 95% (p-value < 0.05). The desirability function in RSM was used to optimize parameters.[36] The desirability method is based on turning all of the collected responses from different scales into a scale-free value. The values of the desirability functions range from 0 to 1. When the factors generate an adverse reaction, the number 0 is assigned, whereas the value 1 represents the ideal performance for the factors evaluated.[37] The optimization objectives can be used to maximize, decrease, or achieve the desired value of the response. The goal of this effort is to maximize the percentages of MGs and DGs.

2.4. Pressure Drop and Mixing Performance. To study the mixing performance of the SMR the pressure drop along the SM was monitored and calculated. The pressure drop was measured with a pressure gauge (PI) installed between the inlet and outlet of SM. The pressure drops in the empty tube and tube with KSM were calculated by using eq 2 based on a resistance coefficient or friction factor in the Darcy−Weisbach equation. Coefficients a and b depend on the Reynolds number (*Re*) and static mixer types. For large values of *Re*, the resistance coefficients a and b are constant.[38] ρ and v are the density and velocity of the fluid, respectively. l and d correspond to the length and diameter of the mixing tube. The fluid velocity was 0.0223 m/s. The densities of G, FAME, and the mixture were 1,261.3, 868.4, and 1,003.76 kg/m^3, respectively. The viscosities of G, FAME, and the mixture were 0.954, 0.00385, and 0.452 kg/(m·s), respectively.

$$\Delta P = \frac{a}{Re^b}\left(\frac{l}{d}\frac{\rho v^2}{2}\right) \quad (2)$$

2.5. Energy Consumption and Performance Comparison. The performance of SMR on glycerolysis was compared with other types of equipment, including a stirred tank reactor and ultrasonic probe reactor.

The stirred tank reactor had a tank diameter of 0.21 m with a volume of 13 L and a pitched blade turbine diameter of 0.15 m. The stirring speed was 200 rpm. The temperature was kept constant with a heater controller.

The ultrasonic probe reactor was a 500 mL three-neck flask. The probe was a titanium sonotrode with a length of 100 mm and a diameter of 22 mm diameter. The ultrasonic processor UP400S, Hielscher, Germany, was operated at 24 kHz and 400 W. The temperature was kept constant by the heater controller.

Energy consumptions (E) per unit mass product gain by SMR, stirred tank reactor, and ultrasonic probe reactor operated at the same glycerolysis condition were calculated using eqs 3a, 3b, and 3c, respectively. The energy consumption of each piece of equipment was determined by multiplying its power by the operating time. The percent yield of product and percent FAME conversion are shown in eqs 3e, 3d, and 3e, respectively

$$E_{SMR} = E_{feed\ pump} + E_{hot\ oil\ pump} + E_{vacuum\ pump} + E_{heater} \quad (3a)$$

$$E_{Stirred\ tank\ reactor} = E_{feed\ pump} + E_{hot\ oil\ pump} + E_{vacuum\ pump} + E_{heater} + E_{stirrer} \quad (3b)$$

$$E_{Ultrasonic} = E_{feed\ pump} + E_{hot\ oil\ pump} + E_{ultransonic} + E_{heater} \quad (3c)$$

$$\%\ yield\ of\ product = \frac{(\%\ purity\ of\ MGs + \%\ Purity\ of\ DGs) \times weight\ of\ product\ phase}{feed\ weight} \times 100 \quad (3d)$$

$$\%\ FAME\ conversion = \frac{initial\ weight\ of\ FAME - final\ weight\ of\ FAME}{initial\ weight\ of\ FAME} \times 100 \quad (3e)$$

2.6. Glycorolysis of Purified Glycerol. The crude glycerol (CG) was purified by a multistep process including acidification, phase separation, neutralization, extraction with hexane, bleaching, filtration, and water evaporation proposed by Tabtimmuang et al.[35] to obtain purified glycerol (PG). Glycerolysis of PG was performed under the condition 3:1 G:FAME mol:mol, 3 wt % KOH, 60 min, and 150 °C.

2.7. Analytical Methods. The MGs, DGs, TGs, FFA, and FAME were analyzed by thin-layer chromatography with flame ionization detection (TLC-FID, IATROSCAN MK-65, Mitsubishi Kagahu Iatron Inc., Tokyo, Japan). To calibrate

https://doi.org/10.1021/acsomega.4c04858
ACS Omega 2024, 9, 39703−39714

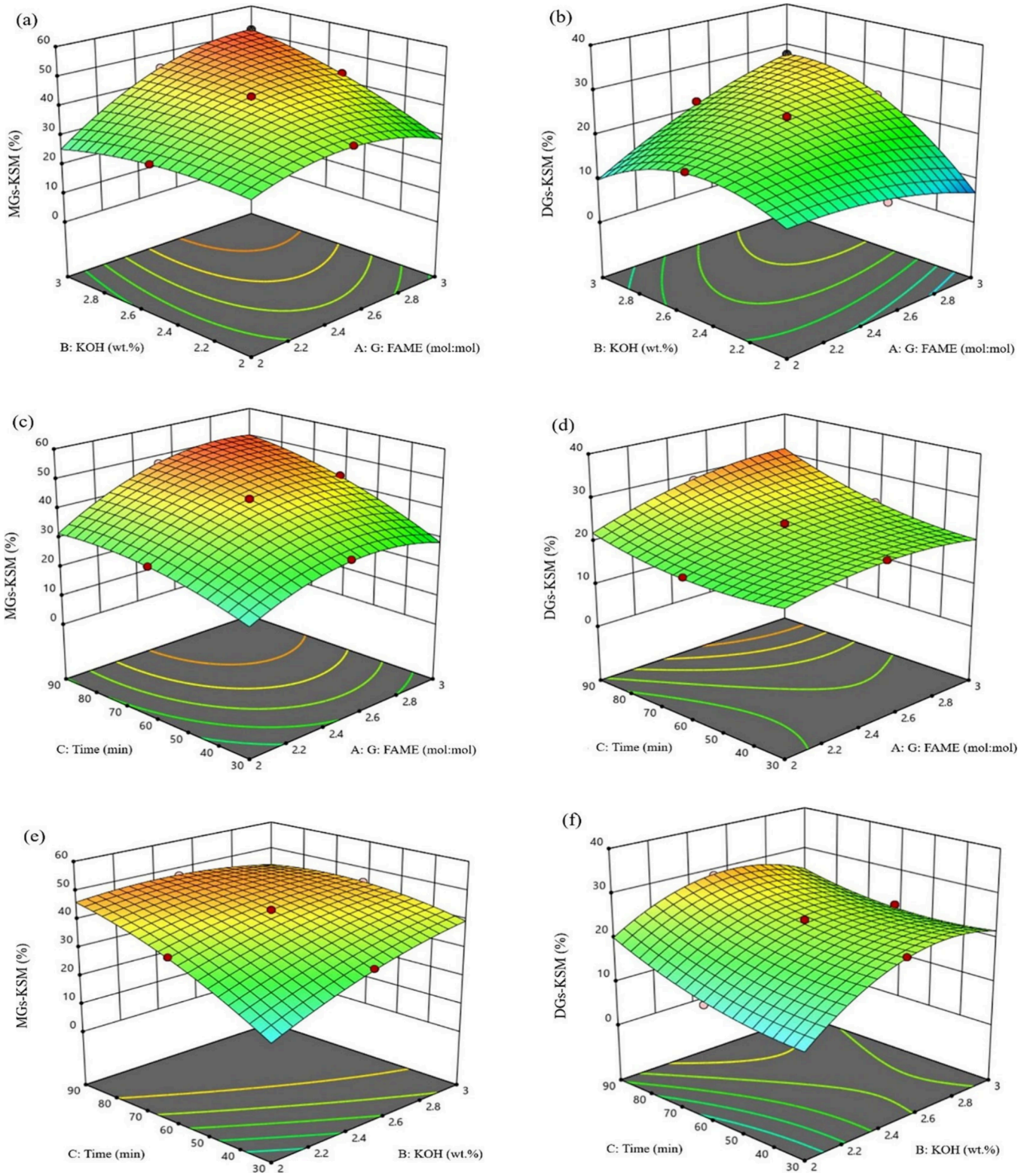

Figure 3. Response surface plots representing effects of (a) molar ratio of G:FAME and % KOH on MGs and (b) on DGs, (c) G:FAME and time on MGs and (d) on DGs, and (e)% KOH and time on MGs and (f) on DGs for KSM.

the TLC/FID instrument, six standard samples, tripalmitin, palmitic acid, and methyl palmitate obtained from Nacala Tesque, Inc., Kyoto, Japan, 1,3-distearin and monopalmitin obtained from Sigma-Aldrich Co, USA, and 99% 1,2-distearin from Research Plus, Inc., USA, were used.[19] The glycerol contents of crude, purified, and commercial glycerol were assessed using the ISO 2879-1975 standard procedure. The water content of glycerol was determined to follow ISO 2098-1972 by using a Karl Fischer titrator. Ash content was determined using an ISO 6245. Matter organic nonglycerol (MONG) was computed using the formula 100 − % glycerol − % ash − % water (ISO 2464).

https://doi.org/10.1021/acsomega.4c04858
ACS Omega 2024, 9, 39703−39714

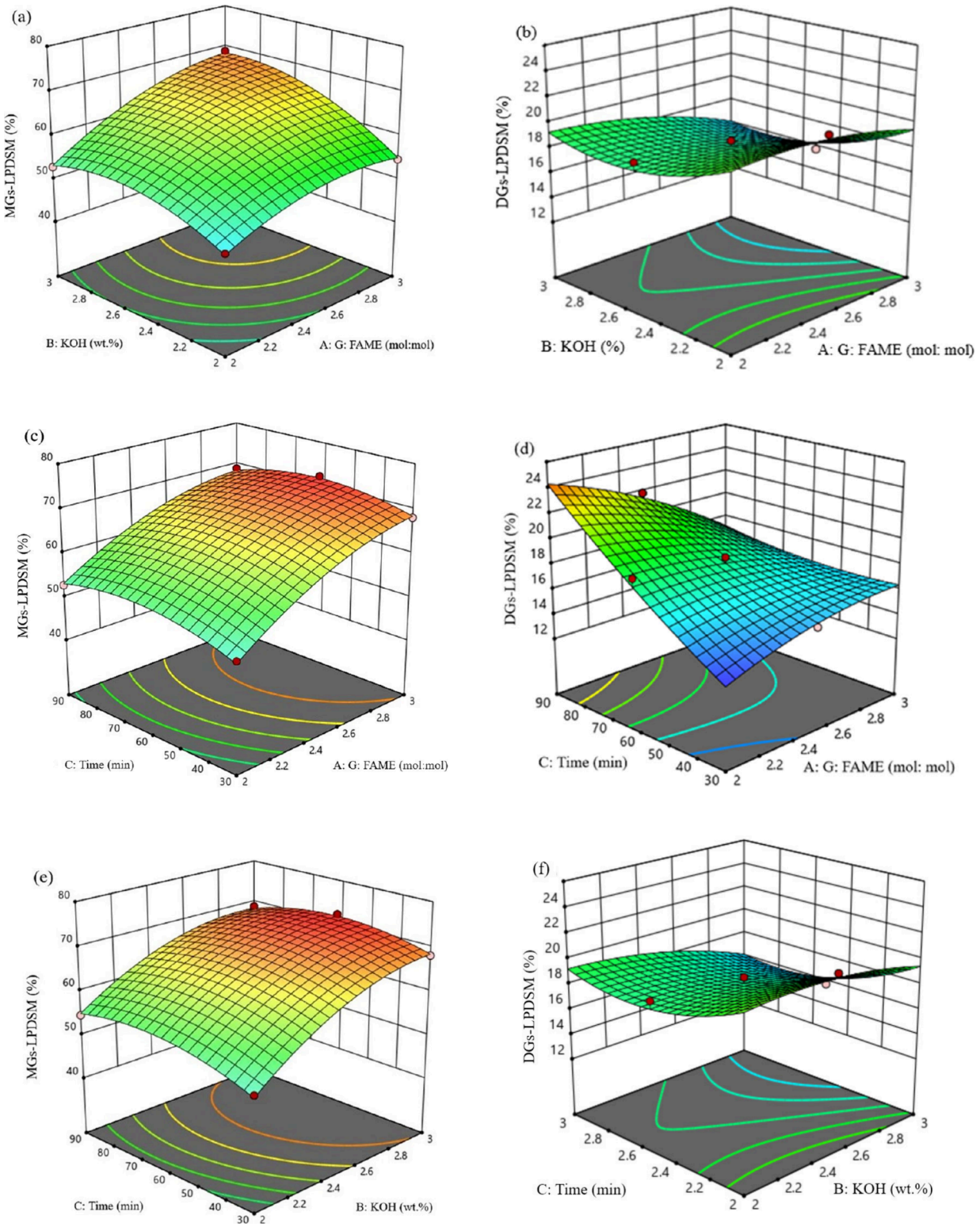

Figure 4. Response surface plots representing effects of (a) molar ratio of G:FAME and % KOH on MGs and (b) on DGs, (c) G:FAME and time on MGs and (d) on DGs, and (e) % KOH and time on MGs and (f) on DGs for LPDSM.

3. RESULTS AND DISCUSSION

3.1. Optimization of Glycerolysis. Variations in the reaction temperature affect the overall kinetic rate constant and glycerol solubility. Therefore, increasing the reaction temperature is predicted to improve the FAME conversion. On the other hand, much higher temperatures cause undesirable breakdown and oxidation processes, resulting in dark products with low yields of the desired grade.[39] In this study, the products were highly viscous at reaction temperatures of 170−215 °C. Separation of residual glycerol and sample analysis was not possible. Glycerolysis at high temperatures can catalyze the polymerization to produce undesirable product formation of polyglycerols on basic catalysts.[40] The products from reaction

https://doi.org/10.1021/acsomega.4c04858
ACS Omega 2024, 9, 39703−39714

Table 2. Developed Equations and Analysis of Variance for the Quadratic Models for MGs and DGs

$$\text{MGs-LPDSM}(\%) = 65.33 + 6.06X_1 + 5.39X_2 + 1.53X_3 + 2.22X_1X_2 - 0.65X_1X_3 - 0.90X_2X_3 - 3.26X_1^2 - 4.09X_2^2 - 3.22X_3^2 \quad (4)$$

$$\text{DGs-LPDSM}(\%) = 18.12 - 1.09X_1 - 1.19X_2 + 2.86X_3 - 0.46X_1X_2 - 2.45X_1X_3 + 0.48X_2X_3 - 0.72X_1^2 + 1.50X_2^2 + 0.48X_3^2 \quad (5)$$

$$\text{MGs-KSM}(\%) = 43.44 + 6.16X_1 + 4.44X_2 + 7.67X_3 + 6.77X_1X_2 + 3.09X_1X_3 - 5.55X_2X_3 - 6.68X_1^2 - 2.71X_2^2 - 3.43X_3^2 \quad (6)$$

$$\text{DGs-KSM}(\%) = 23.32 + 2.66X_1 + 4.16X_2 + 3.38X_3 + 6.33X_1X_2 + 2.01X_1X_3 - 1.75X_2X_3 - 2.27X_1^2 - 6.35X_2^2 - 2.31X_3^2 \quad (7)$$

MGs-LPDSM				DGs-LPDSM		
Source	P-value	F-value	R^2	P-value	F-value	R^2
Models	<0.0001	246.35	0.9955	<0.0001	79.86	0.9863
X_1	<0.0001	693.77		<0.0001	51.31	
X_2	<0.0001	549.84		<0.0001	61.58	
X_3	<0.0001	41.82		<0.0001	333.31	
X_1X_2	<0.0001	75.61		0.0209	7.50	
X_1X_3	0.0347	5.97		<0.0001	195.35	
X_2X_3	0.0067	11.60		0.0205	7.56	
X_1^2	<0.0001	54.37		0.0339	6.04	
X_2^2	<0.0001	85.82		0.0004	26.58	
X_3^2	<0.0001	60.10		0.1077	3.12	
Lack of Fit	0.6138	0.8052		0.4892	1.09	
MGs-KSM				DGs-KSM		
Source	P-value	F-value	R^2	P-value	F-value	R^2
Models	<0.0001	1918.15	0.9995	<0.0001	124.23	0.9920
X_1	<0.0001	2692.30		<0.0001	83.58	
X_2	<0.0001	1399.97		<0.0001	204.13	
X_3	<0.0001	4174.00		<0.0001	135.27	
X_1X_2	<0.0001	2603.46		<0.0001	378.95	
X_1X_3	<0.0001	542.84		0.0002	38.18	
X_2X_3	<0.0001	1751.54		0.0004	29.02	
X_1^2	<0.0001	865.57		0.0028	16.62	
X_2^2	<0.0001	142.57		<0.0001	130.31	
X_3^2	<0.0001	228.33		0.0025	17.24	
Lack of Fit	0.1703	2.80		0.6404	0.7238	

temperatures of 140−160 °C in this study were not too viscous. A temperature of 150 °C giving the highest MGs was then selected to study the effects of other parameters. The experimental results and predicted values of MGs and DGs for both KSM and LPDSM are shown in Table 1. Both static mixers produced higher MGs than DGs under all testing conditions. This is due to the glycerolysis reaction producing more dominant MGs than DGs.

The effect of the G:FAME molar ratio and % KOH, G:FAME and time, and % KOH and time on the production of MGs and DGs for KSM are illustrated by the three-dimensional RSM plot as shown in Figure 3. Increasing both G:FAME molar ratio and % KOH resulted in high MG concentrations (Figure 3a). Similarly, raising both the G:FAME molar ratio and time gave prominent MGs (Figure 3c). When the reaction time was 30 min, increasing % KOH enhanced production of MGs; however, when the time was 90 min, accelerating % KOH degraded MGs (Figure 3e). When % KOH was 3, raising the G:FAME molar ratio gave high DGs, but when % KOH was 2, high DGs were observed when the G:FAME molar ratio was about 2.6 (Figure 3b). Increasing both G:FAME molar ratio and time boosted DGs (Figure 3d). High DG concentrations were found at a reaction time of 90 min and 2.6% KOH (Figure 3f).

From stoichiometry, a 1:1 molar ratio of G:FAME is required to produce 1 mol of MGs.[17] Glycerolysis is a reversible reaction, and extra glycerol is frequently utilized to drive the reaction forward and achieve large FAME conversions. However, a large amount of glycerol and catalyst can inhibit the reaction.[41] An excessive quantity of catalyst can lead to the formation of side reactions or block the active sites on the catalyst's surface.[42] The undesired byproducts, such as fatty acid esters or other glycerol derivatives, can be produced.[43] Glycerol can dilute the reaction mixture and restrain immoderate interaction between glycerides. Increasing the molar ratio of G:FAME reduces MG's secondary reaction to create DGs. Glycerolysis reaction time is often temperature dependent. When a high temperature is applied, the reaction rate increases while the reaction time decreases. From this study at the temperature 150 °C longer reaction time was required to produce more DGs than MGs.

The effects of the G:FAME molar ratio, % KOH, and time on MGs and DGs for the LPDSM are shown in Figure 4. It was found that the LPDSM produced higher % MGs and %

https://doi.org/10.1021/acsomega.4c04858
ACS Omega 2024, 9, 39703−39714

Table 3. Parameter Optimization and Desirability for Different Targets

SM	Condition	Target	G:FAME (mol:mol)	KOH (wt %)	Time (min)	MGs (%)	DGs (%)	Desirability
LPDSM (L/D = 1.5)	1	Maximize only MGs	3:1	2.97	60.23	71.68	16.08	0.986
	2	Maximize only DGs	2:1	2.03	89.86	49.34	25.79	1.000
	3	Maximize both MGs and DGs	2.42:1	3	90	62.74	22.87	0.728
KSM (L/D = 1.5)	4	Maximize only MGs	2.97:1	2.99	79.09	53.21	30.83	1.000
	5	Maximize only DGs	2.97:1	2.98	86.28	53.18	32.64	1.000
	6	Maximize both MGs and DGs	3:1	2.92	90	53.09	34.27	0.999

DGs in almost all conditions compared with KSM. Except for the condition of a 3:1 G:FAME molar ratio, 3% KOH, and 90 min KSM gave greater % DGs. LPDSM, like KSM, generated high MGs when both the G:FAME molar ratio and the % KOH increased, with the maximum MGs produced at a reaction time of around 60 min. However, to obtain high DGs, a low % KOH, a low G:FAME molar ratio and a long time should be operated. The glycerolysis reaction occurs in three steps. In the first step, MGs are produced, and then in the second step, MGs are reacted with FAME to produce DGs as illustrated in the work by Ferretti et al.[17] Longer reaction times are expected for a high composition of DGs.

Equations 4−7 for MG and DG prediction presented in terms of code values (X_1 = molar ratio, X_2 = % KOH, X_3 = time) are shown in Table 2. All R^2 values are roughly near 1, indicating an excellent fit to the data and showing a high correlation between the actual and predicted values.[44] The p-values of the four models (model p-values < 0.0001) and all the variables in quadratic and interaction terms are significant as the p-values < 0.05.[45] The F-values are higher than F-critical implying the models are significant with the lack of fit of all models not being significant. All linear coefficients have positive signs for the three models: MGs from LPDSM, MGs from KSM, and DGs from KSM, suggesting that molar ratio, % KOH, and time presented positive effects on the production of MGs and DGs by KSM and MGs by LPDSM. The production of DGs by LPDSM shows negative signs for molar ratio and % KOH, but a positive sign for time. There are positive and negative signs for interaction coefficients, reflecting both favorable and adverse effects between the parameters. To produce MGs, the effects of the three parameters were not much different. However, for DGs, the reaction time was the most significant parameter.

Table 3 shows the condition optimization and durability for 6 different targets. The conditions with desirability >0.95 are acceptable.[37] To obtain the greatest MGs, LPDSM provided MGs of 71.68% at the recommended conditions 3:1 G:FAME mol:mol, 2.97 wt % KOH, 60.23 min, and 150 °C. Neji et al.[34] reported the optimum conditions at 200 °C, 0.2% w/w acid-activated montmorillonite, and a glycerol/oleic acid ratio of 3:1 to obtain 71.8% MGs. A molar ratio of 6:1 glycerol to oil at 220 °C was found to be the optimal setting for using waste cooking oil as a feedstock.[16] The validation experiments at the condition 3:1 G:FAME mol:mol, 3 wt % KOH, and 60 min for LPDSM obtained 71.35% MGs and 14.20% DGs. To get greater DGs a longer reaction time was suggested. This concept therefore enables the alteration of the glycerolysis conditions to provide appropriate MGs and DGs.

3.2. Mixing Efficiency and the Pressure Drop. Mixing efficiency is related to the pressure drop. The *Re* values of G, FAME, and mixture were 0.59, 101.09, and 1.08, respectively. The coefficients a = 64 and b = 1 were applied in eq 2 for pressure drop calculation in an empty tube. The estimated pressure drops along the tube without SM considering only G, only FAME, and the mixture are shown in Figure 5. The

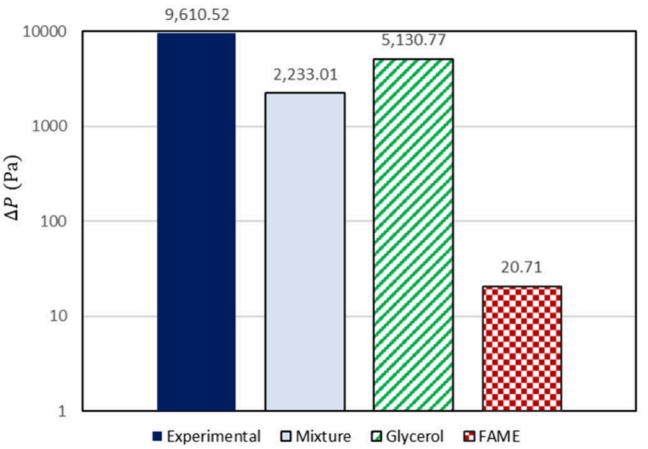

Figure 5. Experimental and estimated pressure drops through the empty tube from glycerolysis with L/D = 1.5, a molar ratio of G:FAME 3:1, 3 wt % KOH, 30 min, and 150 °C.

estimated pressure drop of the glycerol phase is the closest to the measured pressure drop from the experiment. When the static mixer was applied to the same flow condition, the measured pressure drops increased from 9,610.52 Pa in the empty tube (Figure 5) to 24,516.63 Pa (Figure 6). The laminar flow was assumed and checked later. The *Re* of the tube with static mixer (Re_{sm}) can be calculated from eq 8 where ΔP_1 is the pressure drop through the empty tube, ΔP_2 is the pressure drop through the static mixer, and Re_{emp} is the *Re* of the empty tube.

$$Re_{sm} = \Delta P_1 \cdot Re_{emp} / \Delta P_2 \quad (8)$$

The Re_{sm} is approximately 0.39 times the Re_{emp}. Thus, the Re_{sm} values of G, FAME, and mixture were 0.023, 39.42, and 0.42, respectively. Therefore, the laminar flow was still retained in the system with SM. The estimated pressure drops considering each component (G, FAME, or MGs) and the mixture of the flow through KSM were calculated using eq 2 with a = 450 and b = 1 for $Re < 10^{29}$. The predicted pressure drops of the mixture (G, FAME, and MGs) came closest to the experimental pressure drops as shown in Figure 6. This implies that the static mixer enhances the mixing process. However, the experimental pressure drops and estimated pressure drops of the mixture were considerably different. The constants a and b for eq 2 need to be adjusted for this work, in which the Reynolds numbers are between 0.8 and 1.11. From the regression and generalized reduced gradient method for the Solver function in Microsoft Excel the adjusted coefficients are presented in Figure 7a for KSM. The adjusted constants a and b are 3,719.24 and 2.29, respectively, which give the coefficient

https://doi.org/10.1021/acsomega.4c04858
ACS Omega 2024, 9, 39703−39714

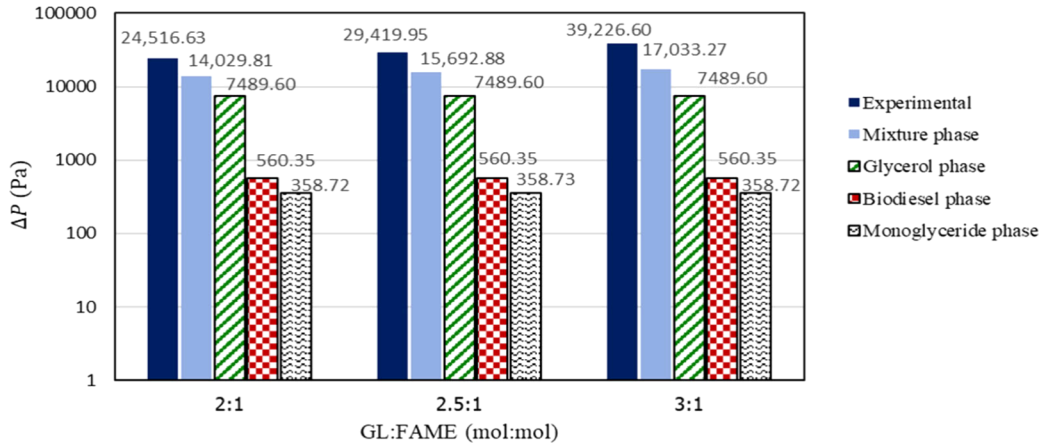

Figure 6. Experimental and estimated pressure drops through KSM (L/D = 1.5) from glycerolysis with different ratios of G:FAME using 3 wt % KOH and reaction time 30 min.

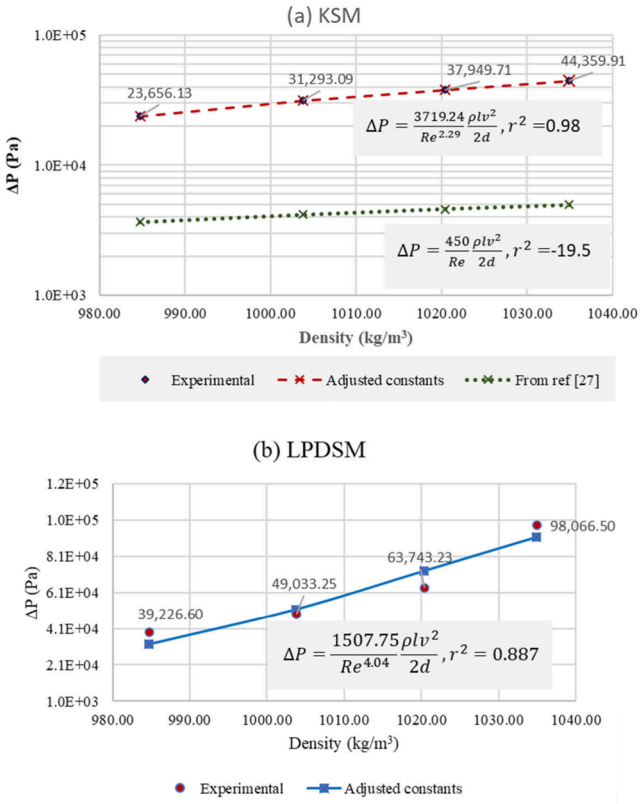

Figure 7. Predicted pressure drop of the static mixer at L/D = 1.5 vs density for (a) KSM and (b) LPDSM.

of determination (R^2) of 0.98. There has been no report on constant values for pressure drop prediction for LPDSM. From this work, the constants a = 1,507.72 and b = 4.04 giving R^2 0.89 were proposed for LPDSM as shown in Figure 7b. The practical condition to provide maximum MGs with a molar ratio of G:FAME 3:1 and 3 wt % KOH for 60 min (Condition 1 using LPDSM in Table 3) was applied to compare the effect of different SM types and L/D ratios on the pressure drops and % MGs. The pressure drop of KSM was lower than that of LPDSM and gave lower % MGs (Table 4). The largest pressure drop was found when LPDSM with L/D = 1.0 was implemented, which yielded the maximum concentration of 79.28% MGs. Lower L/D represents a higher number of

Table 4. Pressure Drops and MGs from Glycerolysis with a Molar Ratio of G:FAME 3:1, 3 wt % KOH, and 60 min

Type of equipment	Length-to-diameter ratio (L/D)	Pressure drop (Pa)	MGs (%)	DGs (%)
Empty Tube	-	9,610.5	-	
KSM	1.5	39,226.6	51.03	31.21
LPDSM	1.0	107,873.2	79.28	10.17
	1.5	63,745.3	71.35	14.20

mixing elements in the same tube length. Thus, the flow pattern is more complex and induces higher mixing performance and reaction conversion.

3.3. Energy Consumption and Performance Comparison. The optimum conditions to obtain the maximum MGs produced by SMR using LPDSM (L/D = 1) were G:FAME molar ratio of 3:1, 3 wt % KOH, 60 min, and 150 °C. This condition was also applied to the stirred tank reactor (STR). It was found that feeding 2.64 kg of G and 2.88 kg of FAME (or total feed of 5.52 kg) gave FAME conversion of 95.52% and 3.76 of kg product phase using SMR and 3.15 kg using the STR. The same glycerolysis condition using the ultrasonic probe reactor gave 50.9% MGs,[35] which is lower than those obtained from SMR as shown in Table 4. If the suggested condition from RSM for the ultrasonic probe reactor was applied (G:FAME molar ratio of 2.82:1, 3.18 wt % KOH, 155.66 °C, and 46.33 min, this condition utilized 0.285 kg of reactants in a 500 mL reactor and gave 0.156 kg of product with 53.32% MGs.[35] All yields, purities of MGs and DGs, and energy consumptions are shown in Table 5. The SMR with LPDSM gave a higher yield of product and MG purity while consuming less energy per product of MGs and DGs compared to the stirred tank reactor and ultrasonic probe reactor due to its passive mixing mechanisms and the absence of the moving components requiring energy consumption.

In the STR, energy is primarily concentrated on the drawing vortices formed behind the blade turbine. Achieving equilibrium between breakup and coalescence in the STR is time-consuming.[46] Consequently, the energy cost of operation in the STR is relatively higher compared to that of the SMR. The energy consumption per kilogram of product for the ultrasonic probe reactor is quite high since the reactor is tiny in comparison to the reactor size of the SMR and stirred tank reactors. For a more accurate comparison of energy usage, the same-sized reactor should be operated. However, it is obvious

https://doi.org/10.1021/acsomega.4c04858
ACS Omega 2024, 9, 39703−39714

Table 5. Performance Comparison of SMR with LPDSM, a Stirred Tank Reactor, and an Ultrasonic Probe Reactor

Type of equipment	% Yield	MGs (%)	DGs (%)	P (W)	$Time_{operation}$ (min)	E (kJ/kg MGs and DGs)	E (kJ/kg MGs)
SMR (LPDSM, L/D = 1.0)	68.12	79.28	10.17	20.93	60	21,803.46	24,600.39
Feed pump				12	60	12,844.45	14,492.13
Hot oil pump				0.75	30	401.39	452.88
Heater				0.37	30	198.02	223.42
Vacuum pump				7.81	60	8,359.60	9,431.96
STR	49.57	65.02	21.85	21.13	60	27,061.78	36,156
Feed pump				12	60	15,787.14	21,092.41
Hot oil pump				0.75	30	493.35	659.14
Heater				0.37	30	243.39	325.17
Vacuum pump				7.81	60	10,274.79	13,727.64
Stirrer				0.2	60	263.12	351.54
Ultrasonic probe reactor[35]	32.92	53.32	15.67	1.9	60	40,627.37	52,567.19
Ultrasonic (24 Hz)				0.4	46.33	11,850.82	15,333.61
Heater				1.5	30	28,776.55	37,233.57

that the SMR performs better in glycerolysis since it yielded more product and has greater MG purity.

3.4. Glycorolysis of Purified Glycerol. The chemical compositions and physical properties of crude glycerol, purified glycerol, and commercial glycerol are listed in Table 6. The crude glycerol is composed of 49.72% glycerol, major impurities of 42.73% matter organic nonglycerol (MONG), and minor contaminants of 5.6% ash and 1.95% water. The purified glycerol contains 95% glycerol with 2.10% MONG while the commercial glycerol used in this study consists of >99.00% glycerol. The purity of glycerol is determined by the grade. Glycerol of 95% purity is technical glycerol, which is used as a building block for chemical manufacturing; 96%−99% glycerol purity is USP-grade glycerol, which is utilized in food and pharmaceutical goods, and 99.7% glycerol purity is Kosher glycerol, which is used to make Kosher food.[47] The purified glycerol meets the purity defined for technical glycerol. Glycerolysis was performed under conditions 3:1 G:FAME mol:mol, 3 wt % KOH, 60 min, and 150 °C. The glycerolysis using purified glycerol gave an acceptable 61.09% MGs and 23.44% DGs when compared to the glycerolysis of commercial glycerol, which obtained 79.28% MGs and 10.17% DGs. The lower obtained MGs from using purified glycerol were from lower glycerol in the source and the water in purified glycerol caused hydrolysis reactions of FAME or G.[48]

Table 6. Chemical Composition and Physical Properties of CG, PG, and Commercial Glycerol

Sample	Crude glycerol	Purified glycerol	Commercial glycerol
Glycerol (wt %)	49.72	94.71	>99.00
Ash (wt %)	5.60	1.29	0.00
Water (wt %)	1.95	1.90	0.97
MONG (wt %)	42.73	2.10	0.00
pH	9.38	5.76	5.50
Density (g/cm^3 at 20 °C)	1.0332	1.2575	1.2613
Viscosity (cP at 25 °C)	320.41	628.46	954

4. CONCLUSIONS

A static mixer coupled with a reactor tank offered better mixing performance to enhance the glycerolysis reaction to produce MGs and DGs while consuming less energy per unit mass of product than a stirred tank reactor and ultrasonic probe reactor. The optimum conditions of glycerolysis to obtain a maximum MG of 79.28 were G:FAME molar ratio of 3:1, 3 wt % KOH of G, 60 min, and 150 °C using the low-pressure drop static mixer with L/D of 1. If a high amount of DGs is required, a longer reaction time is recommended. The lower L/D ratio of LPDSM enhanced the mixing process and gave a higher pressure drop. The new coefficients a and b for the equation to estimate pressure drops in SMR with KSM and LPDSM for glycerolysis were proposed. The production yields of MGs and DGs using purified glycerol were lower than those obtained with pure glycerol but still acceptable. This effort will be beneficial for the utilization of crude glycerol generated during biodiesel production and will make the process more valuable.

AUTHOR INFORMATION

Corresponding Author

Kulchanat Prasertsit − *Department of Chemical Engineering, Faculty of Engineering, Prince of Songkla University, Hat Yai, Songkhla 90110, Thailand;* orcid.org/0000-0003-0719-6264; Email: kulchanat.k@psu.ac.th

Authors

Pakamas Chetpattananondh − *Department of Chemical Engineering, Faculty of Engineering, Prince of Songkla University, Hat Yai, Songkhla 90110, Thailand*

Athcharaporn Tabtimmuang − *Department of Chemical Engineering, Faculty of Engineering, Prince of Songkla University, Hat Yai, Songkhla 90110, Thailand*

Complete contact information is available at: https://pubs.acs.org/10.1021/acsomega.4c04858

Notes

The authors declare no competing financial interest.

ACKNOWLEDGMENTS

This research was financially supported by the National Science, Research and Innovation Fund (NSRF) and Prince of Songkla University (Grant No. ENG6601022b), Hat Yai, Songkhla, Thailand. We thank the Specialized R&D Center for Alternative Energy from Palm Oil and Oil Crops, Department of Chemical Engineering, Faculty of Engineering, PSU, for providing all materials, facilities, and supporting staff to accomplish this work.

https://doi.org/10.1021/acsomega.4c04858
ACS Omega 2024, 9, 39703−39714

REFERENCES

(1) Kowalska-Kuś, J.; Held, A.; Nowińska, K. A continuous-flow process for the acetalization of crude glycerol with acetone on zeolite catalysts. *Chemical Engineering Journal* **2020**, *401*, 126143.

(2) Veljković, V. B.; Banković-Ilić, I. B.; Stamenković, O. S. Purification of crude biodiesel obtained by heterogeneously-catalyzed transesterification. *Renewable and Sustainable Energy Reviews* **2015**, *49*, 500−516.

(3) Anitha, M.; Kamarudin, S. K.; Kofli, N. T. The potential of glycerol as a value-added commodity. *Chemical Engineering Journal* **2016**, *295*, 119−130.

(4) Echeverri, D. A.; Cardeno, F.; Rios, L. A. Glycerolysis of crude methyl ester with crude glycerol from biodiesel production. *J. Am. Oil Chem. Soc.* **2013**, *90*, 1041−1047.

(5) Ferrero, G. O.; Sánchez-Faba, E. M.; Eimer, G. A. Two products one catalyst: Emulsifiers and biodiesel production combining enzymology. *nanostructured materials engineering and simulation models, Chemical Engineering Journal* **2018**, *348*, 960−965.

(6) Silva, T. F. C. V.; Peri, P.; Fajardo, A. S.; Paulista, L. O.; Soares, P. A.; Martínez-Huitle, C. A.; Vilar, V. J.P. Solar-driven heterogeneous photocatalysis using a static mixer as TiO2-P25 support: Impact of reflector optics and material. *Chemical Engineering Journal* **2022**, *435*, 134831.

(7) *Expert Market Research, Mono Diglycerides Market Size, Share, Analysis, Industry Trends*. Accessed: Apr. 24, 2023. [Online]. Available: https://www.expertmarketresearch.com/reports/mono-diglycerides-market.

(8) *Data Bridge Market Research. Mono and Diglycerides and Derivatives Market Scope by 2030*. Accessed: October, 2023. [Online]. Available: https://www.databridgemarketresearch.com/reports/global-mono-and-diglycerides-and-derivatives-market.

(9) Partridge, D.; Lloyd, K. A.; Rhodes, J. M.; Walker, A. W.; Johnstone, A. M.; Campbell, B. J. Food additives: Assessing the impact of exposure to permitted emulsifiers on bowel and metabolic health − introducing the FADiets study. *Nutr Bull.* **2019**, *44* (4), 329−349.

(10) Kamel, B. S. Emulsifiers. *Food Additive User's Handbook* **1991**, 169−201.

(11) Orthoefer, F.; Kim, D. Applications of Emulsifiers in Baked Foods. *Food Emulsifiers and Their Applications*, 3rd ed.; Springer: 2019; pp 299−321, .

(12) Alvarez Serafini, M. S.; Tonetto, G. M. Synthesis of glycerides of fatty acids by inorganic solid catalysts: A Review. *ChemBioEng. Review* **2022**, *9* (1), 110−123.

(13) Hermida, L.; Abdullah, A. Z.; Mohamed, A. R. Synthesis of monoglyceride through glycerol esterification with lauric acid over propyl sulfonic acid post-synthesis functionalized SBA-15 mesoporous catalyst. *Chemical Engineering Journal* **2011**, *174* (2−3), 668−676.

(14) Temelli, F.; King, J. W.; List, G. R. Conversion of oils to monoglycerides by glycerolysis in supercritical carbon dioxide media. *J. Am. Oil Chem. Soc.* **1996**, *73* (6), 699−706.

(15) Ferreira-Dias, S.; Fonseca, M. M. R. Production of monoglycerides by glycerolysis of olive oil with immobilized lipases: effect of the water activity. *Bioprocess Eng.* **1995**, *12* (6), 327−337.

(16) Mamtani, K.; Shahbaz, K.; Farid, M. M. Glycerolsys of free fatty acids: A review. *Renewable and Sustainable Energy Review.* **2021**, *137*, 110501.

(17) Ferretti, C. A.; Olcese, R. N.; Apesteguía, C. R.; Di Cosimo, J. I. Heterogeneously-catalyzed glycerolysis of fatty acid methyl esters: Reaction parameter optimization. *Ind. Eng. Chem. Res.* **2009**, *48* (23), 10387−10394.

(18) Ghanem, A.; Lemenand, T.; Della Valle, D.; Peerhossaini, H. Static mixer: Mechanisms applications, and characterization methods − A review. *Chem. Eng. Res. Des.* **2014**, *92* (2), 205−228.

(19) Somnuk, K.; Prasit, T.; Prateepchaikul, P. Effects of mixing technologies on continuous methyl ester production: Comparison of using plug flow, static mixer, and ultrasound clamp. *Energy Conversion and Management* **2017**, *140*, 91−97.

(20) Bacci di Capaci, R.; Doneddu, M.; Brunazzi, E.; Pannocchia, G.; Galletti, C. CFD Analysis of Inline Mixing of Non-Ideal Liquid Mixtures. *Chemical Engineering Transactions* **2023**, *100*, 325−330.

(21) Nyande, B. W.; Thomas, K. M.; Lakerveld, R. CFD analysis of a Kenics static mixer with a low pressure drop under laminar flow conditions. *Ind. Eng. Chem. Res.* **2021**, *60* (14), 5264−5277.

(22) Kumar, V.; Shirke, V.; Nigam, K. D. P. Performance of Kenics static mixer over a wide range of Reynolds number. *Chemical Engineering Journal* **2008**, *139* (2), 284−295.

(23) Somnuk, K.; Soysuwan, N.; Prateepchaikul, G. Continuous process for biodiesel production from palm fatty acid distillate (PFAD) using helical static mixers as reactors. *Renewable Energy* **2019**, *131*, 100−110.

(24) Galaktionov, O. S.; Anderson, P. D.; Peters, G. W. M.; Meijer, H. E. H. Analysis and Optimization of Kenics Static Mixers. *Int. Polym. Process.* **2003**, *18* (2), 138−150.

(25) Jiang, X.; Xiao, Z.; Jiang, J.; Yang, X.; Wang, R. Effect of element thickness on the pressure drop in the Kenics static mixer. *Chemical Engineering Journal* **2021**, *424* (23), 130399.

(26) Díez, A. M.; Moreira, F. C.; Marinho, B. A.; Espindola, J. C.A.; Paulista, L. O.; Sanromán, M. A.; Pazos, A.; Boaventura, R. A. R.; Vilar, V. J. P. A step forward in heterogeneous photocatalysis: Process intensification by using a static mixer as catalyst support. *Chemical Engineering Journal* **2018**, *343*, 597−606.

(27) Myers, K. J.; Janz, E. E.; Cathie, N. M.; Jones, A. Employ static mixers for process intensification, American Institute of Chemical Engineer. *Chemical Engineering Process* **2018**, *114* (3), 55−62.

(28) Kolmetz, K. Static mixer selection, sizing and troubleshooting (Engineering Desing Guideline). *Kolmetz Handbook of Process Equipment Design*. 2014. www.klmtechgroup.com.

(29) Kumar, V.; Shirke, V.; Nigam, K. D. P. Performance of Kenics static mixer over a wide range of Reynolds number. *Chemical Engineering Journal.* **2008**, *139* (2), 284−295.

(30) Mahammedi, A.; Ameur, H.; Ariss, A. Numerical investigation of the performance of Kenics static mixers for the agitation of shear-thinning fluids. *Journal Of Applied Fluid Mechanics* **2017**, *10* (3), 989−999.

(31) Shishir, M. R. I.; Chen, W. Trends of spray drying: A critical review on drying of fruit and vegetable juices. *Trend in Food Science & Technology* **2017**, *65*, 49−67.

(32) Baixiaofeng, Z. Z. Comparison about the three central composite designs with simulation. *International Conference on Advanced Computer Control*; IEEE Computer Society: Singapore, 2009; pp 163−167, DOI: 10.1109/ICACC.2009.48.

(33) Satyawali, Y.; Cauwenberghs, L.; Maesen, M.; Dejonghe, W. Lipase catalyzed solvent free synthesis of monoacylglycerols in various reaction systems and coupling reaction with pervaporation for *in situ* water removal. *Chemical Engineering and. Processing* **2021**, *166*, 108475.

(34) Neji, S. B.; Chaari, A.; Galán, M. L.; Frikha, F.; Bouaziz, M. Application of box-Behnken design in production of monoglyceride with esterification of glycerol and oleic acid. *ACS Omega* **2023**, *8* (31), 28813−28820.

(35) Tabtimmuang, A.; Prasertsit, K.; Kungsanant, S.; Kaewpradit, P.; Chetpattananondh, P. Ultrasonic-assisted synthesis of mono- and diacylglycerols and purification of crude glycerol derived from biodiesel production. *Industrial Crops & Products* **2024**, *208*, 117891.

(36) Amdoun, R.; Khelifi, L.; Khelifi-Slaoui, M.; Amroune, S.; Asch, M.; Assaf-ducrocq, C.; Gontier, E. The desirability optimization methodology: a Tool to Predict Two Antagonist Responses in Biotechnological Systems: Case of Biomass Growth and Hyoscyamine Content in Elicited Datura starmonium Hairy Roots. *Iranian Journal of Biotechnology* **2018**, *16* (1), 11−19.

(37) Alhajabdalla, M.; Mahmoud, H.; Nasser, M. S.; Hussein, I. A.; Ahmed, R.; Karami, H. Application of response surface methodology and box-Behnken design for the optimization of the stability of fibrous dispersion used in drilling and completion operations. *ACS Omega* **2021**, *6* (4), 2513−2525.

https://doi.org/10.1021/acsomega.4c04858
ACS Omega 2024, 9, 39703−39714

(38) Abu-Ghazala, A. H.; Abdelhady, H. H.; Mazhar, A. A.; El-Deab, M. S. Valorization of hazard waste: Efficient utilization of white brick waste powder in the catalytic production of biodiesel from waste cooking oil via RSM optimization process. *Renewable. Energy* **2022**, *200*, 1120−1133.
(39) Gole, V. L.; Gogate, P. R. Intensification of glycerolysis reaction of higher free fatty acid containing sustainable feedstock using microwave irradiation. *Fuel Process. Technol.* **2014**, *118*, 110−116.
(40) Feuge, R. O.; Bailey, A. E. Modification of vegetable oils - VI. The practical preparation of mono- and diglycerides. *Oil & Soap* **1946**, *23* (8), 259−264.
(41) Ferreira-Dias, S.; Correia, A. C.; Baptista, F. O.; da Fonseca, M. M. R. Contribution of response surface design to the development of glycerolysis systems catalyzed by commercial immobilized lipases. *Journal of Molecular Catalysis B: Enzymatic* **2001**, *11* (4), 699−711.
(42) Tsakoumis, N. E.; Rønning, M.; Borg, Ø.; Rytter, E.; Holmen, A. Deactivation of cobalt-based Fischer−Tropsch catalysts: A review. *Catalyst Today* **2010**, *154* (3−4), 162−182.
(43) Ferrero, G. O.; Sánchez-Faba, E. M.; Eimer, G. A. Two products one catalyst: Emulsifiers and biodiesel production combining enzymology. *nanostructured materials engineering and simulation models, Chemical Engineering Journal* **2018**, *348*, 960−965.
(44) Ngige, G. A.; Ovuoraye, P. E.; Igwegbe, C. A.; Fetahi, E.; Okeke, J. A.; Yakubu, A. D.; Onyechi, P. C. RSM optimization and yield prediction for biodiesel produced from alkali-catalytic transesterification of pawpaw seed extract: Thermodynamics, kinetics, and Multiple Linear Regression analysis. *Digital Chemical Engineering* **2023**, *6*, 100066.
(45) Chiedu, O. C.; Ovuoraye, P. E.; Igwegbe, C. A.; Tahir, M. A.; Okeke, J. A.; Egwuatu, C.; Ngige, G. A.; Onyechi, P. C. Central composite design optimization of the extraction and transesterification of tiger nut seed oil to biodiesel. *Process Integration and Optimization for Sustainability* **2024**, *8*, 503−521.
(46) Theron, F.; Le Sauze, N.; Ricard, A. Turbulent Liquid−Liquid Dispersion in Sulzer SMX Mixer. *Ind. Eng. Chem. Res.* **2010**, *49* (2), 623−632.
(47) Salic, A.; Kucan, K. Z.; Gojun, M.; Rogosic, M.; Zelic, B. Chapter 7 − Biodiesel purification: real-world examples, case studies, and current limitations. *In Sustainable Biodiesel* **2023**, 185−237.
(48) Guo, Z.; Xu, X. Lipase-catalyzed glycerolysis of fats and oils in ionic liquids: A further study on the reaction system. *Green Chem.* **2006**, *8* (1), 54−62.

https://doi.org/10.1021/acsomega.4c04858
ACS Omega 2024, 9, 39703−39714